International Geology Review
Publication details, including instructions for authors and subscription information:
http://www.tandfonline.com/loi/tigr20

U-Pb zircon geochronology, geochemical, and Sr-Nd isotopic constraints on the age and origin of basaltic porphyries from western Liaoning Province, China

Guangying Feng [a b], Shen Liu [a], Hong Zhong [a], Caixia Feng [a], Ian M. Coulson [c], Youqiang Qi [a], Yuhong Yang [a b] & Chaogui Yang [a b]

[a] State Key Laboratory of Ore Deposit Geochemistry, Institute of Geochemistry, Chinese Academy of Sciences, Guiyang, 550002, PR China

[b] Graduate University of the Chinese Academy of Sciences, Beijing, 100049, PR China

[c] Solid Earth Studies Laboratory, Department of Geology, University of Regina, Regina, SK, S4S 0A2, Canada

Published online: 21 Nov 2011.

To cite this article: Guangying Feng, Shen Liu, Hong Zhong, Caixia Feng, Ian M. Coulson, Youqiang Qi, Yuhong Yang & Chaogui Yang (2012) U-Pb zircon geochronology, geochemical, and Sr-Nd isotopic constraints on the age and origin of basaltic porphyries from western Liaoning Province, China, International Geology Review, 54:9, 1052-1070, DOI: 10.1080/00206814.2011.605837

To link to this article: http://dx.doi.org/10.1080/00206814.2011.605837

International Geology Review
Vol. 54, No. 9, July 2012, 1052–1070

Taylor & Francis
Taylor & Francis Group

U–Pb zircon geochronology, geochemical, and Sr–Nd isotopic constraints on the age and origin of basaltic porphyries from western Liaoning Province, China

Guangying Feng[a,b], Shen Liu[a]*, Hong Zhong[a], Caixia Feng[a], Ian M. Coulson[c], Youqiang Qi[a], Yuhong Yang[a,b] and Chaogui Yang[a,b]

[a]*State Key Laboratory of Ore Deposit Geochemistry, Institute of Geochemistry, Chinese Academy of Sciences, Guiyang 550002, PR China;* [b]*Graduate University of the Chinese Academy of Sciences, Beijing 100049, PR China;* [c]*Solid Earth Studies Laboratory, Department of Geology, University of Regina, Regina, SK S4S 0A2, Canada*

(*Accepted 11 July 2011*)

Basaltic porphyries from the northeast North China craton (NCC) provide an excellent opportunity to examine the nature of their mantle source and the secular evolution of the underlying mantle lithosphere. In addition, the study helps to constrain the age and the mechanism of NCC lithospheric destruction. In this paper, we report geochronological, geochemical, and Sr–Nd isotopic analyses of a suite of mafic lavas. Detailed laser ablation–inductively coupled plasma–mass spectrometry (LA–ICP–MS) zircon U–Pb dating yielded an age of 223.3 ± 1.1 million years, which we regard as representing the crystallization age of the basaltic porphyries. The bulk-rock analysed samples are enriched in both large ion lithophile elements (LILEs) (i.e. Ba, Sr, and Pb) and light rare earth elements (LREEs), but depleted in high field strong elements (HFSEs) (i.e. Nb, Ta, Zr, Hf, and Ti) and heavy rare earth elements (HREEs), without significant Eu anomalies ($Eu/Eu^* = 089–0.98$). The basaltic porphyries have undergone low degrees (~5%) of partial melting of a garnet-bearing lherzolite mantle. The rocks display very uniform ($(^{87}Sr/^{86}Sr)_i$ (0.70557–0.70583) and negative ε_{Nd} (t) values (–11.9 to –10.1). These features indicate that the western Liaoning basaltic porphyries were derived from a common enriched lithosphere mantle that had previously been metasomatized by fluids related to subduction of Palaeo-Asian sedimentary units. However, the mafic melts were not affected to a significant degree by crustal contamination. Based on earlier studies, these findings provide new evidence that the northeast margin of the NCC had undergone a phase of post-orogenic extensional tectonics during the Middle Triassic. Furthermore, lithospheric thinning occurring across the northern NCC might have been initiated during Early Triassic times and was likely controlled by the final closure of the Palaeo-Asian Ocean, as well as the collision of Mongolian arc terrenes with the NCC.

Keywords: major and trace elements; Sr–Nd isotopes; basaltic porphyries; early Mesozoic; western Liaoning Province; northeast North China craton

1. Introduction

The North China Craton (NCC) is widely believed to have undergone extensive destruction and modification during both the Mesozoic and Cenozoic Eras (Griffin *et al.* 1998; Wu *et al.* 2005; Xu 2001; Ji *et al.* 2008; Wu *et al.* 2008; Zhai 2008a, 2008b; Gao 2009; Xu *et al.* 2009; Zhang 2009a, 2009b; Zheng 2009; Zheng and Wu 2009; Zhu and Zheng 2009; Liu *et al.* 2010a). These geological activities thereby led to dramatic changes in the structure and nature of the NCC. Specifically, the composition of the lithospheric mantle changed from old, cratonic, and enriched to young, oceanic, and depleted (Zhou *et al.* 2005; Zhou 2006). However, the mechanism, timing, range, and dynamic setting of this destruction, as well as the status of the lithosphere prior to destruction, remain contentious (Wu *et al.* 2008; Zheng 2009). Mantle-derived mafic magmas that erupted across the NCC resulted from considerable extension of the continental lithosphere. According to a number of researchers, an investigation of these rift-related mafic rocks can provide invaluable information concerning the process of continental extension, the nature of their mantle source, and the time–space and evolution of this area of lithosphere mantle (e.g. Hall 1982; Windley 1984; Li *et al.* 1997; Zhou *et al.* 1998; Liu *et al.* 2004, 2006). Previous studies on the Sr–Nd–Pb isotopic nature of the mafic rocks (which are principally basalt and gabbro) in the NCC found that the lithosphere mantle is heterogeneous but regular in terms of temporal and spatial distribution (Xu *et al.* 2004; Zhai *et al.* 2004; Zhang *et al.* 2004; Zhou *et al.* 2005; Zhai 2008b). However, most of these studies focused only on the Luxi, Jiaodong, and Taihang Mountain regions. Mesozoic intermediate-acid volcanic rocks are widespread in western Liaoning Province (Zhou *et al.* 2001; Yang

*Corresponding author. Email: liushen@vip.gyig.ac.cn

ISSN 0020-6814 print/ISSN 1938-2839 online

http://dx.doi.org/10.1080/00206814.2011.605837
http://www.tandfonline.com

2007).Therefore, previous studies mainly focused on high-Sr low-Y andesites rather than on basalts (Li *et al.* 2001; Zhang *et al.* 2003; Gao *et al.* 2004). The Mesozoic volcanic rocks in this area can be divided into four major periods: Xinglonggou Formation (176.6 Ma), Lanqi Formation (166–148 Ma), Yixian Formation (132–120 Ma), and Zhanglaogong Formation (~106 Ma) (Zhang *et al.* 2005a, 2006a; Yang 2007). Thus, studies of these Jurassic and Cretaceous rocks provide an excellent opportunity to investigate the evolution of the underlying lithospheric mantle and to present the constraints on the NCC lithosphere thinning process (Yang and Li 2008). Nevertheless, detailed studies are still required because recent studies suggested that magmatic activities occurring in the Triassic are also significant (Zhang *et al.* 2009). In this article, we provide geochronological and geochemical data on the basaltic porphyries from western Liaoning Province of the NCC. U–Pb dating of zircon by laser ablation–inductively coupled plasma–mass spectrometry (LA–ICP–MS) methods showed that these rocks were formed during the Middle Triassic (223 Ma). This study will help us further investigate the properties of Mesozoic lithospheric mantle beneath the NCC, understand the regional tectonic evolution of the lithosphere mantle, and limit the initial age and the mechanism of the lithosphere thinning.

2. Geological background and petrology

Western Liaoning Province lies in the northern margin of the NCC (Figure 1). This area is enveloped by the Archaean craton in the south and the Palaeozoic Xingmeng Orogenic Belt (XMOB) to the north. The XMOB was formed through the assemblage of the NCC and Siberian Plates. In Palaeozoic times, northeastern China represented a collage of three microcontinental blocks (Ye *et al.* 1994; Wu *et al.* 1995), namely, the Jiamusi Block in the east, the Songliao Block in the centre, and the Xing'an Block in the northwest. The three blocks are separated by the Mudanjiang and Nenjiang Faults. Relative investigations indicated that the assemblage of the Jiamusi and Songliao Blocks occurred during the Silurian (HBGMR 1993). The Jiamusi–Songliao Composite Block was accreted to the Xing'an Block along the Nenjiang Fault during the Late Devonian and Early Carboniferous, when the Xingmeng Orogenic Belt was formed (Ye *et al.* 1994; Wu *et al.* 2000). Recent studies suggested that the NCC and Xingmeng Block were amalgamated before the Late Permian times, and then subsequently collided with the Siberian Plate when the Mongolia–Okhotsk Ocean closed (Zhao *et al.* 1990).

The NCC is one of the oldest Archaean cratons in the world; the most ancient dating record concerning the NCC basement can be traced to 3.8 Ga (Liu *et al.* 1992). Its cratonization occurred during the early Proterozoic, and this area was covered during the middle–late Proterozoic and the Palaeozoic by thick sedimentary deposits (Chen and Chen 1997). The NCC is cut by the Tan-Lu Fault Zone, which is a strike–slip fault from Jurassic to Early Cretaceous times (Zhu *et al.* 2001a), and transformed into an extensional graben during the Late Cretaceous and Tertiary times (Zhu *et al.* 2001b).

Western Liaoning developed over this Precambrian cratonic area; it underwent three stages of development prior to the Mesozoic: the crystalline basement took shape from Archaeozoic to early Proterozoic, an aulacogen developed during middle and late Proterozoic times, and a cratonic stable cover developed during the Palaeozoic. The tectonic evolution of this area was affected by the Palaeo-Asian tectonic domain in early Mesozoic times, whereas it was constrained by the Pacific tectonic domain during the middle and late Mesozoic (Wu *et al.* 2000; Ma and Zheng 2009).

The exposed strata include the following: the Late Jurassic Tuchengzi group (J3t), which contains argillaceous siltstone, silty mudstone, siltstone, and multiple component fine conglomerates; the Yixian Formation of Early Cretaceous age, which is composed of conglomerates, basalt, basaltic andesite, andesite, basanite, and their volcaniclastic equivalents; and Quaternary deposits, such as sandy soil and sandy loam-bearing crushed stone. In addition, a variety of subvolcanic rocks (basaltic porphyrite and andesitic porphyrite) occur within the study area (Figure 1).

The study samples are hypabyssal, basaltic porphyries. These are grey-black, porphyritic-textured basaltic rocks whose principal mineral content is euhedral columnar olivine (0.5–3.0 mm, ~10%). The fine-grained groundmass comprises microcrystalline plagioclase (50–55%), pyroxene (30–35%), and glass. Accessory minerals include magnetite, zircon, and apatite.

3. Analytical methods

3.1. LA–ICP–MS U–Pb dating

Zircon was separated from a single rock sample (>40 kg) (FSG01) using conventional heavy liquid and magnetic techniques at the Langfang Regional Geological Survey, Hebei Province, China. Representative zircon grains were handpicked under a binocular microscope, mounted in an epoxy resin disc, and then polished and coated with a thin film of gold. At the State Key Laboratory of Continental Dynamics, Northwest University, China, zircons were documented with transmitted and reflected light, as well as by cathodoluminescence (CL) methods, to reveal their external and internal structures.

U–Pb dating of zircon was conducted with the aid of LA–ICP–MS techniques at the State Key Laboratory of Geological Processes and Mineral Resources, China University of Geosciences, Wuhan. Detailed operating conditions for the LA system and the ICP–MS instrument and data reduction are given in Liu *et al.* (2008a, 2010c, 2010d). An Agilent ChemStation instrument (Agilent

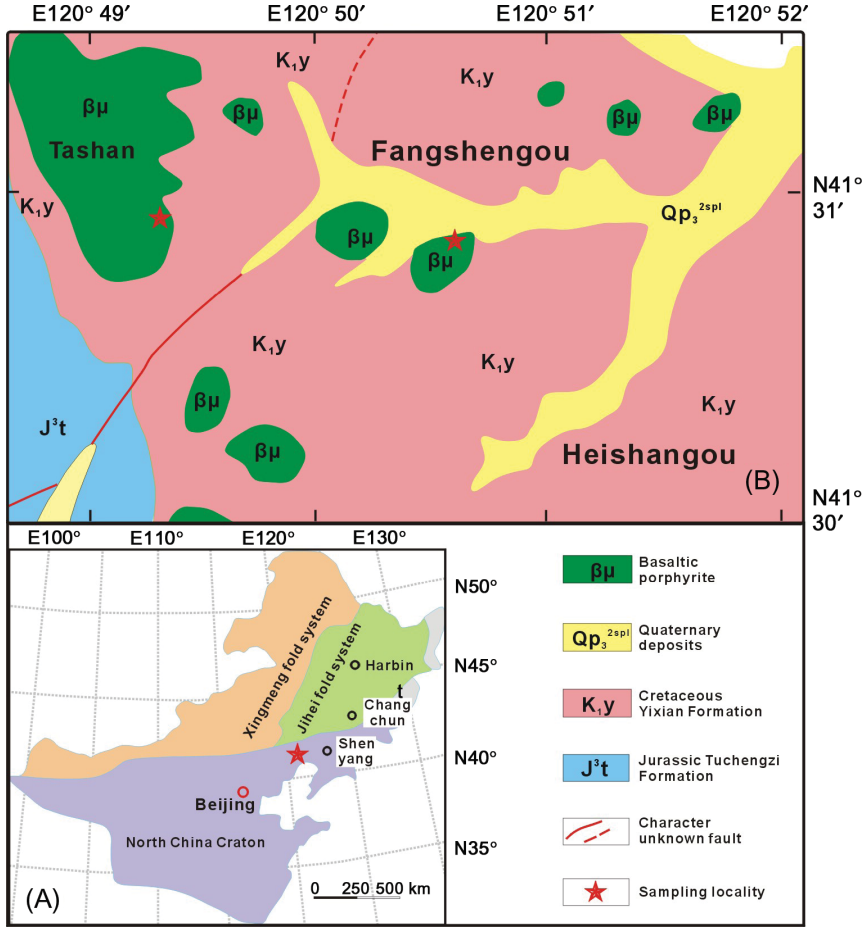

Figure 1. (A) Simplified tectonic map of northeast China and the North China Craton. (B) Geological map of the study area, including the Fangshengou sampling locality for the basaltic porphyries.

Technologies, Inc., Santa Clara, CA, USA) was utilized for the acquisition of each individual analysis. Off-line selection and integration of background and analyte signals, as well as time-drift correction and quantitative calibration for trace element analyses and U–Pb dating, were performed by ICPMSDataCal (Liu *et al*. 2008b, 2010c).

Zircon 91500 was used as an external standard for the U–Pb dating and was analysed twice every five analyses. Preferred U–Th–Pb isotopic ratios used for 91,500 are from Wiedenbeck *et al*. (1995). Uncertainty of preferred values for the external standard 91,500 was propagated to the ultimate results of the samples. Concordia diagrams and weighted mean calculations were made using Isoplot/Ex_ver3 (Ludwig 2003).

3.2. *Major and trace element analyses*

Twelve representative samples were collected to perform major and trace element determinations. Whole-rock samples were trimmed to remove altered surfaces and were cleaned with deionized water, crushed, and powdered with an agate mill.

Major elements were analysed with a Axios-Advanced X-ray fluorescence spectrometer (Axios PW4400; PANalytical B.V., Almelo, The Netherlands) at the State Key Laboratory of Ore Deposit Geochemistry, Institute of Geochemistry, Chinese Academy of Sciences (IGCAS). Fused glass discs were used and the analytical precision, as determined based on the Chinese National Standard GSR-3, was better than 5% (Table 1). Loss on ignition was obtained using 1 g of powder, heated to 1100°C for 1 h.

Trace elements were analysed using a Sciex ELAN 6000 ICP–MS (PerkinElmer, Inc., Waltham, MA, USA) at the IGCAS, China. The powdered samples (50 mg) were dissolved in high-pressure Teflon bombs using a HF+HNO_3 mixture for 48 h at approximately 190°C (Qi and Conrad Grégoire 2002). Rh was used as an internal standard to monitor signal drift during counting. The international standard, GBPG-1, was used for analytical quality control. The analytical precision was generally better than 5% for all elements. Analyses of international standards OU-6 and GBPG-1 are in agreement with recommended values (Table 2).

Table 1. Major oxides (wt. %) of the basaltic porphyries from Fangshengou, western Liaoning Province.

Sample number	SiO_2	TiO_2	Al_2O_3	Fe_2O_3	MgO	CaO	Na_2O	K_2O	MnO	P_2O_5	LOl	Total	Mg#	$Na_2O + K_2O$
FSG-01	49.50	1.64	14.53	11.26	7.99	6.49	3.83	1.09	0.14	1.03	2.13	99.62	61	4.92
FSG-02	49.75	1.65	16.15	11.45	7.89	6.70	3.42	1.74	0.14	0.98	0.69	100.54	60	5.16
FSG-03	50.79	1.73	15.02	11.33	7.87	6.75	4.08	1.34	0.14	0.92	0.45	100.42	60	5.41
FSG-04	49.51	1.63	14.38	11.37	8.20	6.41	3.30	1.99	0.15	1.13	2.01	100.07	61	5.29
FSG-05	50.49	1.73	14.94	11.45	7.95	6.94	4.09	1.14	0.14	0.91	0.71	100.49	60	5.23
FSG-06	49.95	1.68	14.85	11.54	7.75	6.65	3.85	1.22	0.14	1.04	1.74	100.41	60	5.07
FSG-07	49.41	1.66	14.53	11.29	7.91	6.68	3.51	1.59	0.14	1.01	1.97	99.69	61	5.10
FSG-08	49.70	1.65	14.97	11.44	8.23	6.65	3.90	1.11	0.14	1.04	1.45	100.26	61	5.00
FSG-09	49.77	1.66	14.52	11.33	8.01	6.60	3.56	1.54	0.14	1.04	1.80	99.98	61	5.11
FSG-10	49.88	1.67	14.61	11.37	8.12	6.63	3.76	1.24	0.14	1.03	1.61	100.05	61	4.99
FSG-11	49.55	1.66	15.07	11.35	8.07	6.54	3.92	1.10	0.14	1.02	1.49	99.90	61	5.02
FSG-12	50.17	1.67	14.596	11.353	8.09	6.61	3.88	1.10	0.14	1.02	1.58	100.20	61	4.98
GSR3(RV*)	44.64	2.37	13.83	13.40	7.77	8.81	3.38	2.32	0.17	0.95	2.24	99.88		
GSR3(MV*)	44.75	2.35	13.93	13.37	7.73	8.74	3.39	2.29	0.17	0.95	2.24	99.89		
GSR1(RV*)	72.83	0.29	13.40	2.14	0.42	1.55	3.13	5.01	0.06	0.09	0.70	99.62		
GSR1(MV*)	73.27	0.29	13.49	2.14	0.41	1.51	3.13	5.01	0.06	0.09	0.56	99.94		

Note: LOI, loss on ignition; RV*, recommended values; MV*, measured values; $Mg\# = 100 \times \frac{Mg}{Mg + \sum Fe}$ atomic ratio. GSR1 and GSR3 values from Wang *et al.* (2003).

Table 2. Trace elements (ppm) for the basaltic porphyries from Fangshengou, western Liaoning Province.

Sample number	Sc	V	Cr	Co	Ni	Ga	Rb	Sr	Y	Zr	Nb	Ba	La	Ce	Pr	Nd	Sm	Eu	Gd	Tb	Dy	Ho	Er	Tm	Yb	Lu	Hf	Ta	Pb	Th	U	ΣREE	La_N/Yb_N	δEu
FSG-01	16.3	179	271	49.5	189	18.1	4.85	1000	14.8	169	16.0	722	37.3	83.9	10.2	39.1	6.80	1.87	4.96	0.68	3.14	0.63	1.67	0.21	1.26	0.19	4.21	0.75	6.04	2.33	0.58	192	21.2	0.94
FSG-02	14.1	184	251	50.6	191	16.7	13.1	924	13.5	173	16.0	708	33.1	80.0	9.01	34.9	6.22	1.71	4.61	0.61	2.87	0.57	1.43	0.19	1.14	0.16	4.30	0.80	6.19	2.17	0.55	177	20.8	0.94
FSG-03	14.7	169	203	51.7	164	17.0	6.8	906	15.3	184	17.3	667	34.8	79.5	9.39	34.9	6.49	1.74	4.80	0.64	3.14	0.61	1.61	0.22	1.31	0.19	4.31	0.84	5.69	2.54	0.65	179	19.1	0.91
FSG-04	15.6	177	283	45.9	193	18.2	30.9	1080	15.7	177	16.0	798	42.3	92.5	11.2	43.0	7.58	1.97	5.53	0.76	3.40	0.65	1.71	0.22	1.38	0.19	4.67	0.75	6.77	2.69	0.67	212	22.0	0.89
FSG-05	17.6	171	222	53.4	161	18.4	4.34	1030	17.8	185	17.8	730	40.6	88.7	10.7	41.3	7.54	2.05	5.52	0.75	3.65	0.72	1.88	0.23	1.43	0.21	4.41	0.88	6.77	2.99	0.65	205	20.4	0.93
FSG-06	17.5	176	263	47.3	181	18.3	5.54	1060	17.1	172	16.1	765	42.3	89.9	10.9	42.4	7.56	2.02	5.57	0.77	3.67	0.69	1.75	0.22	1.41	0.21	4.21	0.77	6.76	2.78	0.64	209	21.5	0.91
FSG-07	17.9	172	276	48.1	196	18.6	13.9	1070	17.7	174	16.1	744	41.5	90.0	11.4	44.6	7.94	2.24	5.67	0.77	3.63	0.73	1.98	0.26	1.48	0.22	4.17	0.75	6.58	2.97	0.60	212	20.1	0.97
FSG-08	15.1	169	261	49.2	189	17.7	4.75	1040	15.8	167	15.8	734	38.7	86.5	10.3	39.4	7.07	2.02	5.13	0.68	3.35	0.66	1.68	0.21	1.26	0.18	4.13	0.70	6.67	2.57	0.62	197	22.0	0.98
FSG-09	14.8	166	252	46.4	178	17.4	10.8	996	15.4	172	15.8	710	37.5	85.2	10.4	40.6	6.94	1.89	4.93	0.69	3.31	0.61	1.66	0.19	1.20	0.17	4.01	0.71	6.43	2.56	0.60	195	22.4	0.94
FSG-10	14.0	167	241	46.1	180	16.5	5.88	947	14.0	169	15.6	752	34.2	82.6	9.43	36.7	6.56	1.77	4.75	0.66	3.03	0.61	1.57	0.21	1.23	0.17	4.10	0.72	6.59	2.26	0.62	183	19.9	0.92
FSG-11	15.4	167	243	51.5	175	17.3	4.75	1000	15.5	169	15.6	716	37.1	82.1	9.78	38.7	6.83	1.86	5.25	0.69	3.17	0.62	1.59	0.21	1.28	0.20	4.15	0.76	5.96	2.45	0.61	189	20.8	0.91
FSG-12	15.9	168	255	49.4	183	16.6	4.61	981	15.1	168	16.0	734	36.4	82.7	9.51	37.8	6.55	1.87	5.43	0.73	3.38	0.65	1.70	0.21	1.39	0.19	4.25	0.92	7.74	2.56	0.64	189	18.8	0.93
OU-6(RV*)	22.1	129	70.8	29.1	39.8	24.3	120	131	27.4	174	14.8	477	33.0	74.4	7.80	29.0	5.92	1.36	5.27	0.85	4.99	1.01	2.98	0.44	3.00	0.45	4.70	1.06	28.2	11.5	1.96			
OU-6(MV*)	21.8	128	67.3	29.1	38.2	24.7	123	131	28.4	170	15.3	485	33.9	77.6	7.8	30.9	6.19	1.48	5.47	0.87	5.10	1.08	3.08	0.44	2.94	0.46	4.96	1.12	32.0	11.6	2.05			
GBPG-1(RV*)	13.9	96.5	181	19.5	59.6	18.6	56.2	364	18.0	232	9.93	908	53.0	103	11.5	43.3	6.79	1.79	4.74	0.60	3.26	0.69	2.01	0.30	2.03	0.31	6.07	0.40	14.1	11.2	0.90			
GBPG-1(MV*)	13.7	100	171	19.4	55.6	18.7	57.1	358	18.4	255	9.92	899	50.9	96.0	11.1	42.0	6.61	1.78	4.74	0.62	3.18	0.67	2.07	0.28	2.01	0.32	6.18	0.40	13.5	11.3	0.91			

Note: RV*, recommended values; MV*, measured values. The values for GBPG-1 are from Thompson *et al*. (2000) and for OU-6 are from Potts and Kane (2005).

3.3. Sr–Nd isotopic analyses

Whole-rock Sr–Nd isotopic data were obtained using a Finnigan Triton multi-collector mass spectrometer (Thermo Fisher Scientific, Inc., Waltham, MA, USA) at the State Key Laboratory of Geological Processes and Mineral Resources, China University of Geosciences, Wuhan. Sr and Nd isotopic fractionations were corrected to $^{86}Sr/^{88}Sr = 0.1194$ and $^{146}Nd/^{144}Nd = 0.7219$, respectively. During the period of analysis, the NBS987 standard yielded an average $^{87}Sr/^{86}Sr$ value of 0.710215 ± 10 (2σ) and the La Jolla standard gave an average $^{143}Nd/^{144}Nd$ value of 0.511837 ± 1 (2σ). Total procedural Sr and Nd blanks were <4 ng and <1 ng, respectively. Details of the analytical methodology applied are given in Zhang *et al.* (2004).

4. Results

4.1. Zircon U–Pb dating

Sufficient zircon grains were selected from the basaltic porphyry (FSG01) for the analysis. The grains are euhedral, colourless, transparent, and mostly elongate-prismatic, ranging up to 100 μm in diameter. Most zircons exhibit oscillatory or planar zoning under CL excitation, a typical feature of magmatic zircon. Selected zircon CL images are given in Figure 2. The zircon samples have variable abundances of Th (247–1,336 ppm) and U (352–814 ppm) and provide Th/U ratios of 0.7–1.64 (Table 3). These data further showed a magmatic origin for these zircons. The U–Pb zircon dates for these samples are presented in Table 3. Analyses of zircon grains with oscillatory structures were concordant and yielded a weighted mean $^{206}Pb/^{238}U$ age of 223.3 $\pm$ 1.1 million years (see Figure 2). This age was interpreted as the crystallization age of the basaltic porphyries.

4.2. Major and trace elements

The major element concentrations of the studied basaltic porphyries are listed in Table 1. They exhibit low SiO_2 (49.41–50.79 wt.% oxide) and relatively high alkali contents ($Na_2O + K_2O = 4.92$–5.29 wt.% oxides). In the total alkali-silica diagram (Figure 3), all the volcanic rock samples fall within the field of the alkaline rock series. Moreover, the volcanic rocks are characterized by high concentrations of MgO (7.75–8.23%, Mg# = 60–61). Positive correlations were observed in the plots of MgO versus P_2O_5, Cr, and Ni, whereas negative correlations were observed in the plots of MgO versus SiO_2, TiO_2, CaO, and Zr. In addition, MgO and Al_2O_3 display a weak negative correlation.

The trace element compositions of the samples are presented in Table 2. Total REE ranges from 177 to 212 ppm. All samples are characterized by significant enrichment in light rare earth elements (LREEs) and strong depletion in heavy rare earth elements (HREEs) with $(La/Yb)_N = 19.1$–22.4. The samples lack significant Eu anomalies ($Eu/Eu^* = 089$–0.98) (Figure 4A). The basaltic porphyries

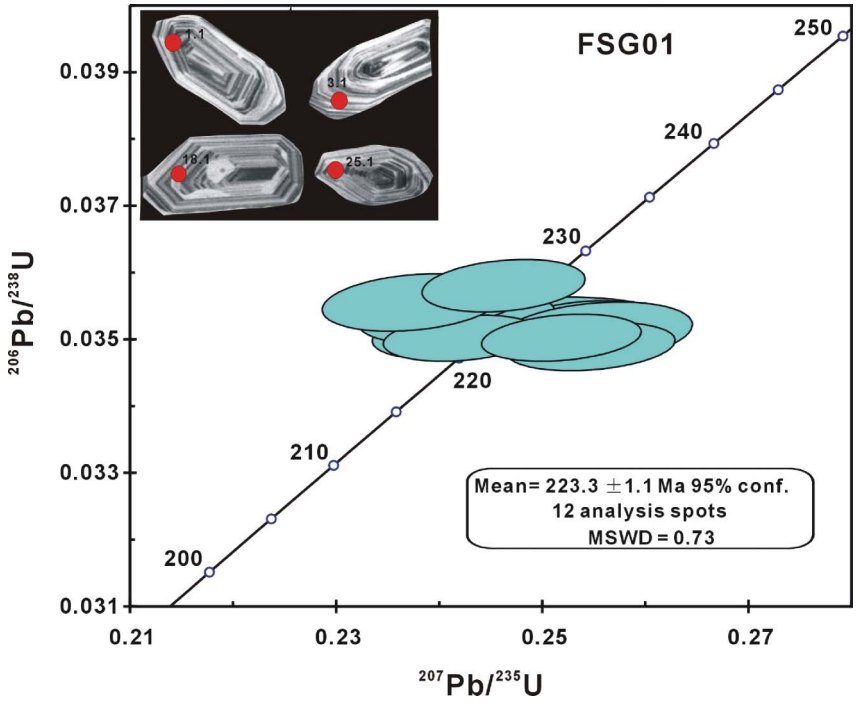

Figure 2. Representative cathodoluminescence images and LA–ICP–MS U–Pb Concordia diagrams for zircon grains from the basaltic porphyry samples (FSG01). Note: LA–ICP–MS, laser ablation–inductively coupled plasma–mass spectrometry.

Table 3. LA–ICP–MS U–Pb isotopic data for zircons from the studied basaltic porphyries (FSG01).

FSG01					Isotopic ratios						Age (Ma)					
Spot	Th (ppm)	U (ppm)	Pb (ppm)	Th/U	$^{207}Pb/^{206}Pb$	1σ	$^{207}Pb/^{235}U$	1σ	$^{206}Pb/^{238}U$	1σ	$^{207}Pb/^{206}Pb$	1σ	$^{207}Pb/^{235}U$	1σ	$^{206}Pb/^{238}U$	1σ
1.1	316	362	42.8	0.87	0.0514	0.0023	0.2490	0.0106	0.0352	0.0003	260	80	226	9	223	2
2.1	629	569	76.2	1.10	0.0521	0.0012	0.2540	0.0064	0.0352	0.0003	288	42	230	5	223	2
3.1	376	392	49.8	0.96	0.0497	0.0013	0.2415	0.0062	0.0353	0.0003	181	43	220	5	223	2
4.1	395	427	51.4	0.92	0.0496	0.0012	0.2405	0.0058	0.0351	0.0003	178	41	219	5	222	2
5.1	721	655	90.5	1.10	0.0493	0.0015	0.2415	0.0078	0.0353	0.0003	161	58	220	6	224	2
6.1	310	371	40.8	0.84	0.0526	0.0016	0.2550	0.0077	0.0351	0.0004	313	49	231	6	222	2
7.1	310	387	44.1	0.80	0.0490	0.0014	0.2400	0.0066	0.0356	0.0003	148	47	218	5	225	2
8.1	1336	814	150	1.64	0.0500	0.0012	0.2420	0.0062	0.0350	0.0003	196	45	220	5	222	2
9.1	346	418	46.8	0.83	0.0530	0.0014	0.2546	0.0067	0.0349	0.0003	330	44	230	5	221	2
10.1	247	352	34.3	0.70	0.0485	0.0014	0.2372	0.0071	0.0356	0.0004	122	52	216	6	225	2
11.1	501	447	64.2	1.12	0.0499	0.0013	0.2461	0.0065	0.0358	0.0003	190	45	223	5	227	2
12.1	434	450	55	0.96	0.0522	0.0013	0.2517	0.0064	0.0350	0.0003	295	42	228	5	222	2

Notes: LA–ICP–MS, laser ablation–inductively coupled plasma–mass spectrometry. Errors are at the 1σ level; Common Pb was corrected using the method proposed by Andersen (2002).

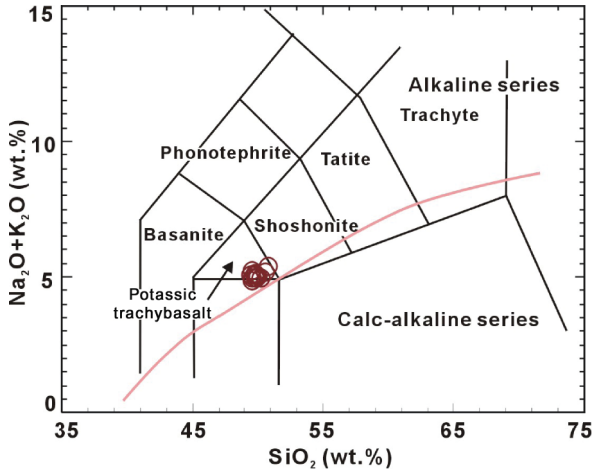

Figure 3. Total alkali-silica diagram for the Fangshengou basaltic porphyries.

have high Cr (203–283 ppm), Co (45.9–53.4 ppm), and Ni (161–196 ppm) contents, consistent with their high MgO contents. In addition, when plotted on primitive mantle normalized multi-element diagrams (Figure 4B), the samples exhibit Sr and Ba enrichment, as well as Nb, Ta, Zr, Hf, and Ti depletion.

4.3. *Sr–Nd isotope*

Isotopic data for whole-rock Sr and Nd were obtained from representative basaltic porphyry samples (Table 4). The rock samples display very uniform $^{87}Sr/^{86}Sr$ ratios ranging from 0.705633 to 0.705904, with initial $^{87}Sr/^{86}Sr$ values of 0.705568–0.705827. Moreover, the rocks show only minor variations, as well as low initial $^{143}Nd/^{144}Nd$ = 0.511740–0.511831 and ε_{Nd} (t) = –11.9 to –10.1. Nd isotopic model age (T_{DM}) is an important parameter related to Nd isotopic characteristics. Considering the different degrees of Sm/Nd fractionation, researchers generally accept that only when the value of $f_{Sm/Nd}$ = –0.5 to –0.2 can the model age be considered effective and have geological meaning (Wu *et al.* 1997). The Nd isotopic model ages of the basaltic porphyries range from 1.67 to 1.81 thousand million years, and their corresponding $f_{Sm/Nd}$ vary between –0.46 and –0.43. The results showed that the aforementioned model ages are effective, and they indicated dates relating to the palaeo-Mesoproterozoic.

Previous geochemical studies of mantle-derived magma and deeply derived xenoliths from the NCC clearly demonstrated that the lithospheric mantle is enriched from the Palaeozoic to Mesozoic (Wang *et al.* 1996; Yan *et al.* 2000; Zhou *et al.* 2001). Therefore, the Nd isotopic model ages are thought to record the enrichment time of the NCC lithosphere mantle.

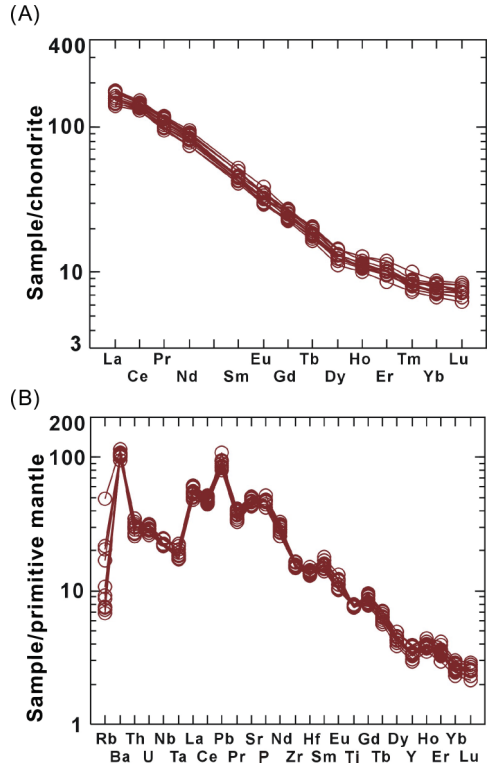

Figure 4. (A) Chondrite-normalized REE patterns and (B) primitive mantle-normalized multi-element diagram for the basaltic porphyry samples (after Sun and McDonough, 1989). Note: REE, rare earth element.

5. Discussion

5.1. *Fractional crystallization*

The basaltic porphyries are derived from a magma that has undergone very low degrees of fractionation, which preserves their primitive, high MgO (MgO = 7.75–8.23%, Mg# = 60–61), Cr (203–283 ppm), Co (45.9–53.4 ppm), and Ni (161–196 ppm) contents (Liu *et al.* 2008a). The positive correlations between MgO and P_2O_5 and Cr and Ni (Figure 5D, 5H, and 5J) suggest that minor clinopyroxene, olivine, and apatite were involved in their fractional crystallization history. A negative correlation between MgO versus TiO_2 and CaO (Figure 5G and 5I) excludes significant fractionation of rutile and orthopyroxene. The weak correlation between Al_2O_3 and MgO (Figure 5E) further indicates that fractionation and/or accumulation of plagioclase and K-feldspar were not important; this observation is also supported by the near-normal behaviour of Eu (Eu/Eu* = 0.89–0.98) (Figure 4A) and by the positive Sr anomaly (Figure 4B) exhibited.

5.2. *Crustal contamination*

Given that the mafic rocks were erupted within a continental environment, these mantle-derived magmas might have been affected by crustal contamination (Mohr

Table 4. Sr–Nd isotopic ratios for the basaltic porphyries from the western Liaoning Province.

Sample number	Rb (ppm)	Sr (ppm)	$^{87}Rb/^{86}Sr$	$^{87}Sr/^{86}Sr$	$\pm2\sigma$	$(^{87}Sr/^{86}Sr)_i$	Sm (ppm)	Nd (ppm)	$^{147}Sm/^{144}Nd$	$^{143}Nd/^{144}Nd$	$\pm2\sigma$	$(^{143}Nd/^{144}Nd)_i$	$\varepsilon Nd(t)$	T_{DM1} (Ga)	$f_{Sm/Nd}$
FSG-02	13.1	924	0.0410	0.705904	10	0.705774	6.22	34.9	0.1077	0.511908	11	0.511751	−11.7	1.78	−0.45
FSG-03	6.80	906	0.0217	0.705852	10	0.705783	6.49	34.9	0.1124	0.511988	12	0.511824	−10.3	1.75	−0.43
FSG-05	4.34	1030	0.0122	0.705833	10	0.705794	7.54	41.3	0.1104	0.511992	12	0.511831	−10.1	1.71	−0.44
FSG-08	4.75	1040	0.0132	0.705869	10	0.705827	7.07	39.4	0.1085	0.511898	11	0.511740	−11.9	1.81	−0.45
FSG-10	6.49	915	0.0205	0.705633	12	0.705568	6.78	36.9	0.1111	0.511980	11	0.511818	−10.4	1.74	−0.44
FSG-11	4.75	1000	0.0137	0.705833	12	0.705789	6.83	38.7	0.1067	0.511976	12	0.511820	−10.4	1.67	−0.46

Notes: CHUR, Chondrite Uniform Reservoir.
$^{87}Rb/^{86}Sr = 0.0847$, $^{87}Sr/^{86}Sr = 0.7045$, $^{147}Sm/^{144}Nd = 0.1967$, $^{143}Nd/^{144}Nd = 0.512638$, CHUR values are used for the calculation. $\lambda_{Rb} = 1.42 \times 10^{-11}$ year^{-1} (Steiger and Jäger 1977); $\lambda_{Sm} = 6.54 \times 10^{-12}$ year^{-1} (Lugmair and Harti 1978).

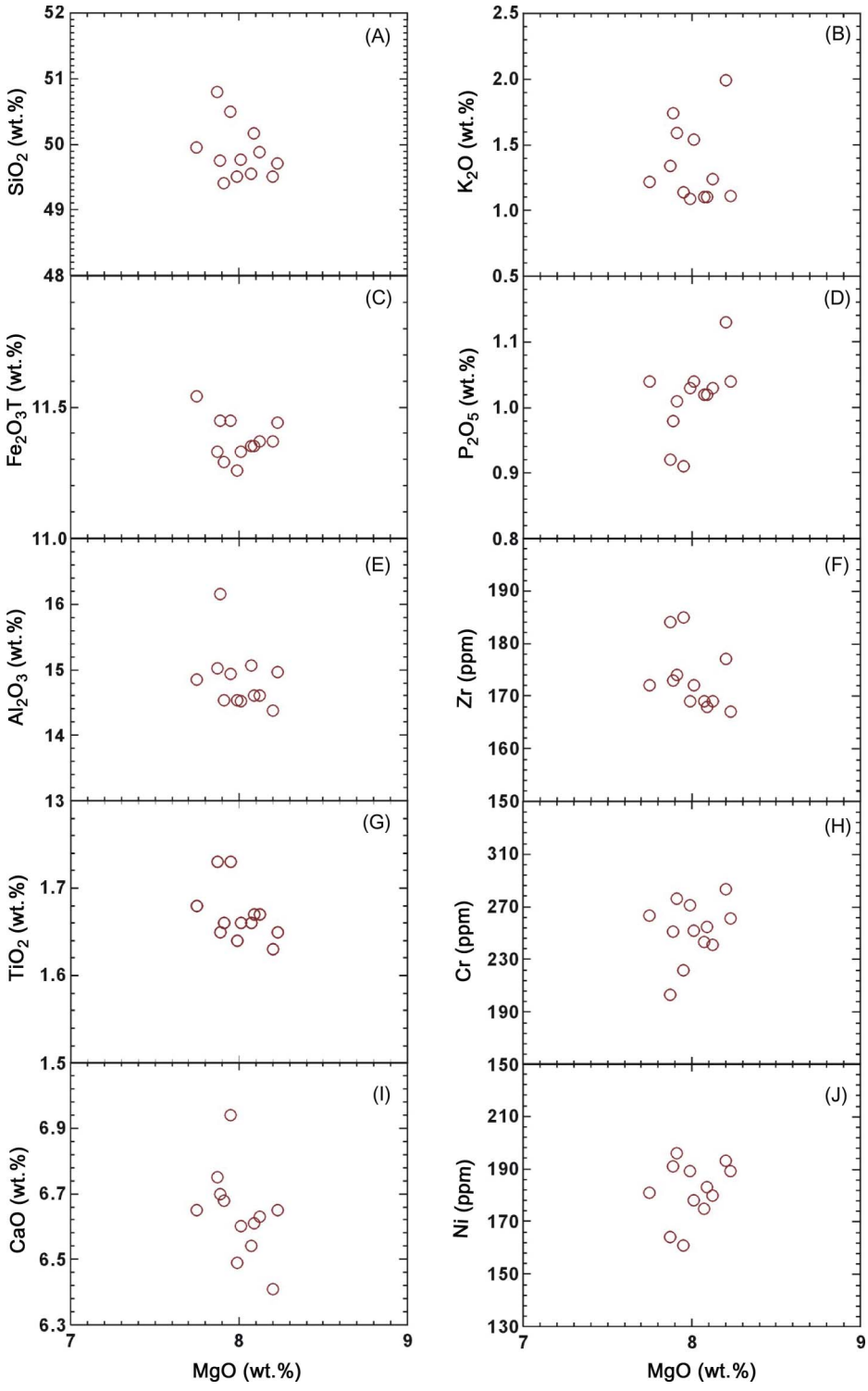

Figure 5. Selected variation diagrams of oxides and trace elements versus MgO of the studied basaltic porphyries. Correlation between MgO and (A) SiO_2, (B) K_2O, (C) Fe_2O_3, (D) P_2O_5, (E) Al_2O_3, (F) Zr, (G) TiO_2, (H) Cr, (I) CaO, and (J) Ni. Note: Ol, olivine; Cpx, clinopyroxene; Pl, plagioclase; Ne, nepheline.

1987). Geochemical characteristics suggest that crustal contamination may have affected the petrogenesis of the western Liaoning Province basaltic porphyries. These characteristics include the significant enrichment in Ba, Sr, and LREE; depletion in HFSE (Nb, Ta, Zr, Hf, and Ti); lower Ta/La (0.02–0.03) and Nb/U ratios (24–29) compared with primitive mantle (e.g. Ta/La = 0.06, Wood *et al.* 1979; Nb/U = 30, Hofmann *et al.* 1986); and

negative $\varepsilon_{Nd}(t)$. However, the volcanic rock samples are characterized by depletion in Th and U relative to La in the primitive mantle-normalized diagrams (Figure 4B), thereby precluding significant contamination by the upper and middle crust (Taylor and McLennan 1985). In the $(^{87}Sr/^{86}Sr)_i$ versus $\varepsilon_{Nd}(t)$ diagram (Figure 6), all the samples deviate from the mantle evolution line and fall in the region of the lower crust. Thus, a likely candidate for the contamination may be the lower crust. Previous investigations of high-temperature and high-pressure granulites in the NCC suggested that lower crust granulites generally have lower Th and U than the similar granulites in other parts of the world (Gao *et al.* 1998; Liu *et al.* 1999). This feature coincides with the depletion in Th and U relative to La in the primitive mantle-normalized diagrams. Accordingly, the Sr content in the melts will decrease following magma differentiation because of the lower Sr abundance of the lower crust rocks (e.g. 46–840 ppm, Jahn and Zhang 1984). In comparison, Sr enrichment is evident in the primitive mantle-normalized diagrams (Figure 4B). Jahn *et al.* (1999) suggested that the $\varepsilon_{Nd}(t)$ for the ancient lower crust is very low (–44 to –32) (Cai *et al.* 2005), which is considerably lower than that for the basaltic porphyry samples (–11.9 to –10.1). Moreover, there is no significant relationship between MgO and either $\varepsilon_{Nd}(t)$ or $(^{87}Sr/^{86}Sr)_i$ (see Figure 7), which is inconsistent with extensive contamination by the lower crust. In summary, the magmatic evolution of the NCC basaltic porphyries in western Liaoning Province was not significantly affected by crust contamination, and the geochemical and isotopic signatures were mainly inherited from an enriched mantle source.

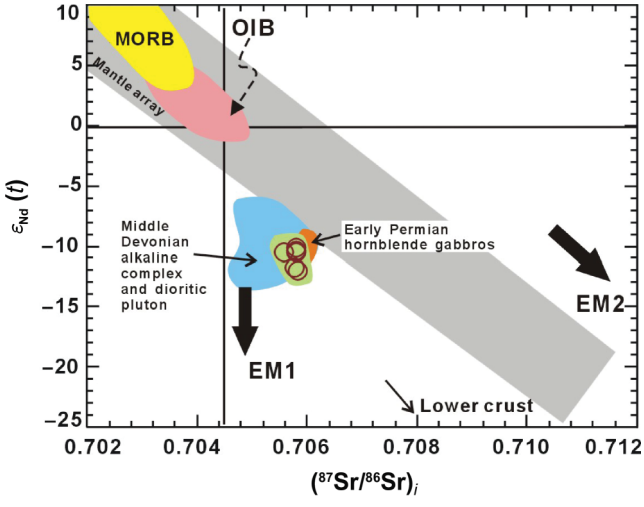

Figure 6. Initial $^{87}Sr/^{86}Sr$ versus $\varepsilon_{Nd}(t)$ diagram for the Fangshengou basalt porphyries. Sr–Nd isotopic compositions of the Ordovician kimberlites and mantle xenoliths in the eastern North China Craton are from Zheng (1999), Zheng and Lu (1999), Wu *et al*. (2006), and Zhang and Yang (2007). Sr–Nd isotopic compositions of the Early Permian hornblende gabbros in the northern NCB are from Zhang *et al*. (in press). MORBs and OIBs are after Zhang *et al*. (2002) and the references therein. Mantle array are from Zhang *et al*. (2005b). Also plotted also trends to lower crust (after Jahn *et al.* 1999). Note: MORB, mid-ocean ridge basalt; OIB, ocean island basalt.

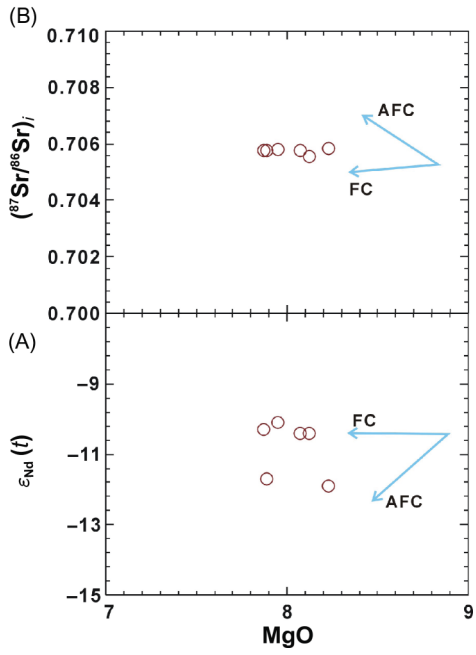

Figure 7. MgO versus $\varepsilon_{Nd}(t)$ (A) and initial $(^{87}Sr/^{86}Sr)$ (B) diagrams of the Fangshengou basaltic porphyries.

5.3. *Source regions and partial melting*

The basaltic porphyries of the western Liaoning Province have low SiO_2 (49.41–50.79%) contents, implying that the rocks came from an ultramafic mantle rather than from the melting of crust (Liu *et al.* 2008a). This observation is further supported by their high Cr and Ni contents (Table 2). Experimental petrology has shown that, with regard to the degree of melting of basalt, melt products/resulting magmas are characterized by low Mg# (<40, Rapp and Watson 1995). The MgO-rich nature (7.75–8.23%) and high Mg# (60–61) signature of the studied basaltic porphyries indicated that these rocks were derived through partial melting of the mantle rather than of the basaltic lower crust. In addition, the negative $\varepsilon_{Nd}(t)$ values (–11.9 to –10.1) (Table 4) for the basaltic porphyry samples indicated that these rocks originated from the partial melting of an enriched lithospheric mantle beneath the NCC rather than from an asthenospheric mantle, such as for mid-ocean ridge basalt. An enriched lithospheric mantle is further supported by the Nd isotopic model age T_{DM} (1.71–1.81 thousand million years). Previous studies in the region have revealed that the Yanshanian mafic rocks in the NCC (western Liaoning and western Shandong) and the Dabie–Sulu orogenic belt were similarly derived from an enriched lithosphere mantle. Nd isotopic model ages (T_{DM}) ranging from 1.4 to 2.0 thousand million years were obtained from these areas,

which are consistent with those of the studied basaltic porphyries from the western Liaoning Province (Chen and Chen 1997; Chen and Jahn 1998; Ma *et al.* 1998; Jahn *et al.* 1999, 2001; Fan *et al.* 2001; Guo *et al.* 2001; Zhou *et al.* 2001).

The REE content of basaltic rocks is chiefly controlled by primary mantle composition and degree of partial melting (e.g. Johnson 1998; Zhao and Zhou 2007; Liu *et al.* 2010b). Based on their partitioning coefficients, the REE contents are moderately incompatible during melting of mantle peridotite (Johnson 1998); therefore, their concentrations and ratios are not significantly affected by mantle depletion and fluid influx (Pearce and Peate 1995; Münker 2000). The Yb ($D_{garnet/melt} = 6.6$) content in primary melts is mainly buffered by residual garnet during the melting of mantle peridotite (Johnson 1998). Thus, the melts produced by partial melting of mantle peridotite with a garnet residue have low Yb concentration and high LREE (e.g. La and Sm/Yb ratio); moreover, garnet has a high partition coefficient for Sm ($D_{garnet/melt} = 0.22$) relative to La ($D_{spinel/melt} = 0.01$) (McKenzie and O'Nions 1991), and for Yb ($D_{garnet/melt} = 6.6$) relative to Sm ($D_{garnet/melt} = 0.25$) (Johnson 1998). By contrast, the partial melts from spinel–lherzolite sources should result in a relatively flat melting trend in terms of REE patterns defined by depleted and enriched source compositions (Green 2006), because spinel has similar partition coefficients for La ($D_{spinel/melt} = 0.01$), Sm ($D_{spinel/melt} = 0.01$), and Yb ($D_{spinel/melt} = 0.01$) (McKenzie and O'Nions 1991). In the Sm/Yb versus Sm plot (Figure 8), the basaltic porphyry samples exhibit higher Sm/Yb ratios for the spinel–lherzolite melting curve but lie close to those of the garnet–lherzolite melting trend, implying a garnet–lherzolite mantle source. Our calculations from trace element geochemistry suggested that the basaltic porphyry samples were formed from melts that underwent low-degree (~ 5%) partial melting of the source (Figure 8). This inference is also supported by the high La/Sm (5.2–5.6) and $(La/Yb)_N$ ratios (19.1–22.4) of these rocks because La/Sm and La/Yb are strongly fractionated when the degree of melting is low. We conclude that the basaltic porphyry samples from western Liaoning Province were generated by low-degree partial melting of an enriched, garnet-bearing lherzolite mantle below the NCC.

5.4. Mantle metasomatism

The basaltic porphyry samples are characterized by enrichment in Ba, Sr, Pb, and LREEs, but depletion in HFSEs. This magma had not experienced extensive crustal contamination. We suggest that the mantle source probably has metasomatized by fluid. There are two main mechanisms for the formation of fluids within the mantle: degasification of the earth and dehydration related to the subduction of oceanic lithosphere (Ding and Sun 2001). Previous studies

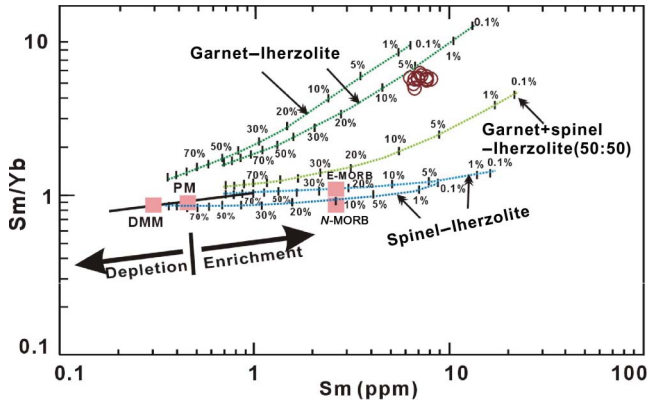

Figure 8. Sm/Yb versus Sm diagram of the Fangshengou basaltic porphyries.

have suggested that the contents of the LILE (i.e. Rb, K, Sr, Ba, U, and Pb) can be intensely affected by melting processes in the mantle wedge above a subduction zone because these elements are strongly soluble in the fluid phase (Regelous *et al.* 1997; Johnson and Plank 1999). By contrast, the high field strength elements (i.e. Nb, Ta, Zr, Hf, and Ti) are depleted because of their weak solubility and relative immobility in these types of fluid. For these reasons, we conclude that the features of the chemical traits exhibited by the basaltic porphyry samples possibly relate to subduction-type fluid metasomatism in their source mantle. In the Mesozoic, the evolution of western Liaoning Province was influenced by the tectonics of the Palaeo-Asian Ocean and the Pacific tectonic domain. Previous studies have indicated that the Palaeo-Asian Ocean began to subduct beneath the NCC at the start of the early Palaeozoic, and then the northern margin of the NCC developed into an Andean-type active continental margin (Zhao *et al*. 2010). It was not until the Late Jurassic to Early Cretaceous that the Pacific Plate began to collide and compress with the Eurasian continent (Ren and Huang 2002), the impact of the Pacific was apparently gradual in this area. On the basis of the timing relationships within the study area, we propose that the mantle source of basaltic porphyries from western Liaoning Province likely experienced metasomatism by fluids derived from the subduction of the Palaeo-Asian Plate and its entrained volcanic and sediment load.

Rb depletion in the primitive mantle-normalized diagram (Figure 4B) can be interpreted as metasomatism of amphibole within the mantle source. Given that the Rb/Sr ratios in amphiboles are lower than or close to the Rb/Sr ratios (~0.03) of the primitive mantle, the presence of amphibole cannot yield whole-rock Rb/Sr ratios higher than those of the primitive mantle (~0.03) (Ionov *et al.* 1997). These results are consistent with the Rb/Sr ratios (0.004–0.029) found in the NCC basaltic porphyry samples.

5.5. Petrogenesis and geodynamic significance

5.5.1. Petrogenesis

In the Palaeoproterozoic, Eastern Europe, Siberia, and the NCC formed a unified continent, which separated during mid- to Neoproterozoic times. The Palaeo-Asian Ocean that lay between Siberia and the NCC formed at approximately 1.4 Ga, followed by a sustained period of expansion (Shi *et al.* 2004). This hypothesis is consistent with the view of Zhao *et al*. (2010), who suggested that the history of the predecessor of the Palaeo-Asian Ocean (Panthalassa) started from at least 1.35 Ga. Oceanic crust existed in the northern NCC throughout the Palaeozoic Sengör *et al.* 1993). Since early Palaeozoic times (∼490 Ma), the Palaeo-Asian Ocean began its southward subduction beneath the NCC, resulting in the development of an active continental margin along the northern edge of the NCC (Chen *et al.* 2000; Shi *et al.* 2004). Ni *et al*. (2004) reported that eclogites from the northern Hebei Province exhibit oceanic crust-like characteristics and that the petrogenetic age of their original protolith lies in the early Palaeozoic (438 Ma). These findings provide further support that the northern margin of the NCC was affected by the subduction of the Palaeo-Asian Ocean from the north during the early Palaeozoic (Tian *et al.* 2007). In the middle and Late Carboniferous, the southward subduction of the Palaeo-Asian Oceanic Plate continued, followed by the development of a mature, Andean-type continental margin along the northern margin of the NCC (Xiao *et al.* 2003; Zhang *et al.* 2006b, 2007a). Meanwhile, a great number of diorite, quartz diorite, and granodiorite plutons were emplaced into the Inner Mongolia uplift related to actively developing arc-type terranes therein (Zhang *et al.* 2007b, 2007c). The time of the final closure of the Palaeo-Asian Ocean is universally recognized as of great importance, both within the academic communities in China and globally. Although this hypothesis is still controversial, a considerable number of supported, multi-disciplinary research endeavours have provided support to the idea that the final collision and amalgamation of the NCC within the Mongolian arc terranes occurred during the Late Permian and the Early Triassic times (Hsu *et al.* 1991; Wang *et al*. 1991; Sengör *et al*. 1993; Zorin *et al*. 1993; Wang and Mo 1995; Chen *et al.* 2000; Xiao *et al.* 2003; Shang 2004; Li 2006; Miao *et al.* 2007; Windley *et al.* 2007; Wu *et al.* 2007; Lin *et al.* 2008; Xiao *et al.* 2009). The final suture for this collision is thought to be situated along the Solon–Xilin (Xilamulun)–Changchun–Yanji line rather than along the Solon–Hengenshan line (Hsu *et al.* 1991; Sengor *et al.* 1993).

Igneous rocks are widely distributed along the northern margin of the NCC. These rocks were emplaced during the Late Permian and Triassic periods. The geochronology of mafic rocks in this area includes the following: a whole-rock Rb–Sr isochron age for a lamprophyre vein outcropping near Datong (229 ± 11 million years) (Shao *et al.* 2003); the timing of basalt magmatic activities in the Inner Mongolia, Kalaqin Banner (237–220 million years) (Shao *et al.* 1999); and a zircon U–Pb age for the Xiaozhangjiakou pyroxenite (220 ± 5 million years) (Tian *et al.* 2007). Alkaline magmatism has also been reported (Yan *et al.* 2000, 2001), with the majority of these ages between 208 and 250 million years (Chen *et al.* 2008). Cai *et al*. (2006) pointed out that the distribution of this early Mesozoic belt of alkaline rocks was along the northern margin of the NCC (i.e. between 104°–127° E longitude and 40°–42° N latitude). Moreover, the high-precision, isotopic ages for this suite of alkaline rocks range from 190 to 250 million years (Mu and Yan 1992; Jing *et al.* 1995; Yan *et al.* 2000; Han *et al.* 2004; Ren *et al.* 2005). This Mesozoic alkaline belt extends for thousands of kilometres along a nearly E–W trend. In this study, it has become clear that in the western Liaoning Province the basaltic porphyrites are relatively high alkaline; their age is 223 ± 1.1 million years; and these rocks lie within the geographical location of the other alkaline rocks forming the belt. These aforementioned authors have noted that in the northern NCC, there occurs a mafic-ultramafic and alkaline magmatic belt (dated at ∼220 Ma) that lies roughly parallel to the final suture of the Palaeo-Asian Ocean (i.e. Solon–Xilin–Changchun–Yanji line) (Chen *et al.* 2008). Hence, the magmatic activities thought to be responsible for this magmatism are believed to be closely related to the closure of the Palaeo-Asian Ocean; these activities relate all the aforementioned magma associations and their geochemical characters to post-collisional/post-orogenic tectonics and extensional magmatism within the northern NCC during early Mesozoic times (Zhao *et al*. 2010).

Based on the preceding discussions, the northern margin of the NCC would have experienced a phase of post-collisional/post-orogenic extensional in the Middle Triassic. We propose a simple model to illustrate the petrogenesis of the basaltic porphyry samples from western Liaoning Province (Figure 9). During the Palaeozoic, the Palaeo-Asian Ocean was undergoing subduction beneath the NCC, and the lithosphere mantle was being enriched by subduction zone fluid metasomatism (i.e. subduction of the Palaeo-Asian sediment). During the Late Permian and Early Triassic, with the final closure of the Palaeo-Asian Ocean, the Mongolian arc terranes amalgamated with the northern margin of the NCC as a result of orogenesis, which induced thickening of the lithosphere. In the Middle Triassic, the northern NCC evolved into a post-collisional/post-orogenic extensional tectonic setting. The characteristics of zircon Hf isotope of the Xiaozhangjiakou ultra-mafic pluton (220 ± 5 Ma) in the northern NCC suggested that the pluton resulted from the reaction and mixing of the enriched lithosphere mantle and the depleted asthenospheric fluid/melt, indicating that the

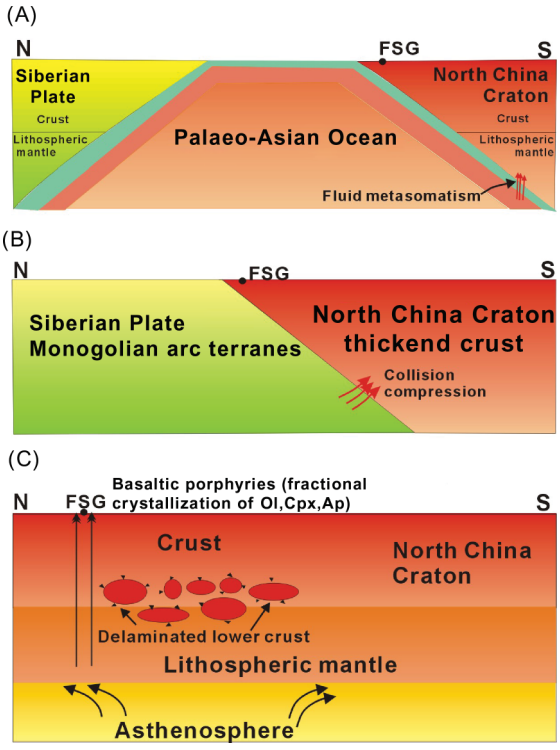

Figure 9. Illustration of tectonic evolution in the northern NCC. (A) In the Palaeozoic, the Palaeo-Asian Ocean subducted below the NCC, thus the lithospheric mantle was 'enriched' by metasomatic subduction-derived fluids from the downgoing Palaeo-Asian sediment. (B) In the Late Permian to Early Triassic, with the final closure of the Palaeo-Asian Ocean, the Mongolian arc terranes amalgamated with the northern NCC and further subducted below the NCC, thereby inducing a thickening of the lithosphere. (C) In the Middle Triassic (~223 Ma), the northern NCC developed into a post-orogenic extensional tectonic environment while the high heat flow of the upwelling asthenosphere triggered low degree partial melting (~5%) of the metasomatized early–middle Proterozoic-enriched lithospheric mantle in the form of a garnet-bearing lherzolite mantle source. Subsequently, this mantle-derived magma (basaltic melting) ascended along fractures and faults to the surface but was not significantly affected by crustal contamination because of rapid ascent. Note: Ol, olivine; CPx, clinoproxene; Ap, apatite; NCC, North China Craton.

asthenosphere of the northern NCC began to rise then. The high heat flow of the upwelling asthenosphere triggered low-degree partial melting (~5%) of the metasomatized early and middle Proterozoic, enriched lithospheric mantle (garnet-bearing lherzolite) in western Liaoning Province. Subsequently, at approximately 223 Ma, these mantle-derived magmas ascended along fractures and faults to the earth's surface and were not significantly affected by crustal contamination. This hypothesis implies that significant extensions had occurred, thinning the lithosphere of the northern NCC (Macdonald *et al.* 2001). During upwelling, fractional crystallization of olivine, clinoproxene, and apatite occurred.

5.5.2. *Tectonic implications*

Studies of mantle xenoliths from Palaeozoic-aged kimberlites, compared with Cenozoic alkali basalts, have proved that some 80–140 km of the ancient cratonic NCC mantle lithosphere was removed following the Ordovician and was replaced by younger, less refractory lithosphere mantle (Menzies *et al.* 1993; Griffin *et al.* 1998; Xu 2001). This activity may have been achieved by thermal–chemical erosion (Menzies *et al.* 1993; Griffin *et al.* 1998; Xu 2001; Zhang *et al*. 2005b) or post-collisional lithosphere delamination (Gao *et al*. 2002, 2004; Wu *et al.* 2003; Yang *et al.* 2003). However, the initiation of lithosphere thinning is still controversial. Menzies *et al*. (1993) and Xu (2001) suggested that removal was caused by indirect tectonics resulting from the collision of India and Eurasia at 40 Ma. Griffin *et al*. (1998) further suggested that lithosphere thinning occurred during the Late Jurassic and Eocene, possibly associated with Mesozoic and Cenozoic subduction. Gao *et al*. (2002) proposed that there was Jurassic lithosphere delamination following collision between the NCC and the Yangtze Craton.

The formation of the basaltic porphyries, as revealed in the current study, showed that lithosphere thinning in western Liaoning province started in the Middle Triassic (~223 Ma). Zhang *et al*. (2009, 2010) implied that the enriched lithosphere mantle in the northern NCC underwent multiple phase deformations before the Triassic, and that the characteristic of the lithosphere mantle became gradually depleted in the Late Triassic. The involvement of the asthenospheric mantle material obviously became significant, indicating that the onset of lithosphere thinning in the northern NCC likely occurred during the Early and Late Triassic. Moreover, the magmatic belt (mainly mafic and alkali rocks) of Triassic age, which is distributed parallel to the suture of the Palaeo-Asian Ocean, suggested that lithosphere thinning in the northern NCC was controlled by the final closure of the Palaeo-Asian Ocean and the subsequent collision of the Mongolian arc terranes and the NCC.

6. Conclusions

On the basis of geochronological, geochemical, and Sr–Nd isotopic analyses, we draw the following conclusions:

(1) U–Pb dating of zircons indicates that the basaltic porphyries were formed at 223.3 ± 1.1 Ma. These rocks are the result of post-collisional/post-orogenic magmatism.
(2) Analytical results further suggest that the basaltic porphyries were derived from a common enriched lithosphere mantle that was metasomatized by subduction zone-type fluids related to the entrained Palaeo-Asian sediment undergoing active subduction beneath the NCC mantle lithosphere.

The parental melts to the western Liaoning Province basaltic porphyries were generated from this enriched lithospheric mantle and subsequently underwent fractional crystallization of olivine, clinopyroxene, and apatite. This magma was not significantly affected by crustal contamination.

(3) We propose that lithosphere thinning throughout the northern NCC occurred during the Early and Late Triassic, controlled by the final closure of the Palaeo-Asian Ocean and the subsequent collision of Mongolian arc terranes against the NCC.

Acknowledgements

This research was supported by the National Nature Science Foundation of China (40773020, 40972071 and 40673029). We are grateful to Lian Zhou for helping with the analysis of Sr and Nd isotopes, and Yongsheng Liu and Zhaochu Hu for help in zircon U-Pb dating.

References

Andersen, T., 2002, Correction of common lead in U-Pb analyses that do not report ^{204}Pb: Chemical Geology, v. 192, p. 59–79.

Cai, J.H., Yan, G.H., and Mu, B.L., 2005, Zircon U-Pb age, Sr-Nd-Pb isotopic compositions and trace element of Fangshan complex in Beijing and their petrogenesis significances: Acta Petrological Sinica, v. 21, p. 776–788.

Cai, J.H., Yan, G.H., and Ren, K.X., 2006, Lithogeochemical characteristics of Early Mesozoic alkaline intrusive rock belt from north margin of North China Craton: Department of Earth Sciences of Nanjing University, ed., The Abstract Collection of 2006 Symposium on Petrology and Geodynamics in China, p. 278–280 (in Chinese).

Chen, B., Jahn, B.M., and Wilde, S., 2000, Two contrasting Paleozoic magmatic belts in northern Inner Mongolia, China: Petrogenesis and tectonic implications: Tectonophysics, v. 328, p. 157–182.

Chen, B., Tian, W., and Liu, A.K., 2008, Petrogenesis of the Xiaozhangjiakou mafic-ultramafic complex, North Hebei: Constraints from petrological, geochemical and Nd-Sr isotopic data: Geological Journal of China Universities, v. 14, no. 3, p. 295–303.

Chen, J.F., and Jahn, B.M., 1998. Crustal evolution of southeastern China: Nd and Sr isotopic evidence. Tectonophysics, v. 284, p.101–133.

Chen, Y.X., and Chen, W.J., 1997. Chronology, geochemistry and setting of Mesozoic volcanic rocks in West Liaoning and adjacent regions: Beijing, Seismological Press, p. 141–201(in Chinese with English abstract)

Ding, Q.F., and Sun, F.Y., 2001, Some progresses in mantle fluid studies: Geological Science and Technology Information, v. 20, no. 3, p. 21–27 (in Chinese with English abstract).

Fan, W.M., Guo, F., Wang, Y.J., Lin, G., and Zhang, M., 2001, Post-orogenic bimodal volcanism along the Sulu Orogenic Belt in eastern China: Physics and Chemistry of the Earth (A), v. 26, p. 733–746.

Gao, S., Luo, T.C., and Zhang, B.R., 1998, Chemical composition of the continental crust as revealed by studies in Eastern China: Geochinica et Cosmochimica Acta, v. 62, p. 1959–1975.

Gao, S., Rudnick, R.L., Carlson, R.W., McDonough, W.F., and Liu, Y.S., 2002, Re-Os evidence for replacement of ancient mantle lithosphere beneath the North China Craton: Earth and Planetary Science Letters, v. 198, p. 307–322.

Gao, S., Rudnick, R.L., Yuan, H.L., Liu, X.M., Liu, Y.S., Xu, W.L., Ling, W.L., Ayers, J., Wang, X.C., and Wang, Q.H., 2004, Recycling lower continent crust in the North China Craton: Nature, v. 432, p. 892–897.

Gao, S., Zhang, J.F., Xu, W.L., and Liu, Y.S., 2009, Delamination and destruction of the North China Craton: Chinese Science Bulletin, v. 54, p. 3367–3378.

Green, N.L., 2006, Influence of slab thermal structure on basalt source regions and melting conditions: REE and HFSE constraints form the Garibaldi volcanic belt, northern Cascadia subduction system: Lithos, v. 87, p. 23–49.

Griffin, W.L., Zhang, A.D., and Reilly, S.Y., 1998, Phanerozoic evolution of the lithosphere beneath the Sino-Korean craton, *in* Flower, M., Chung, S.L., Lo, C.H., and Lee, T.Y., eds., Mantle dynamics and plate interactions in East Asia, Geodynamics Series, Volume 27: Washington, DC, American Geophysics Union, p. 107–126.

Guo, F., Fan, W.M., Wang, Y.J., and Lin, G., 2001, Late Mesozoic mafic intrusive complexes in North China Block: Constraints on the nature of subcontinental lithospheric mantle: Physics and Chemistry of the Earth (A), v. 26, p. 759–771.

Hall, H.C., 1982, The importance and potential of mafic dyke swarms in studies of geodynamic process: Geosciences Canada, v. 9, p. 145–154.

Han, B.F., Kagami, H., and Li, H.M., 2004, Age and Nd-Sr isotopic geochemistry of the Guangtoushan alkaline granite, Hebei province, China: Implications for early Mesozoic crust-mantle interaction in North China block: Acta petrologica Sinica, v. 20, p. 1375–1388 (in Chinese with English abstract).

HBGMR (Heilongjiang Bureau of Geology and Mineral Resources), 1993, Regional Geology of Heilongjiang Province: Beijing, Geological Publishing House, p. 347–438 (in Chinese with English summary).

Hofmann, A.W., Jochum, K.P., Seufert, M., and White W.M., 1986, Nb and Pb in oceanic basalts: New constraints on mantleevolution: Earth and Planetary Science Letters, v. 79, p. 33–45.

Hsu, K.J., Wang, Q., and Hao, J., 1991, Geologic evolution of the Neomonides: A working hypothesis: Eclogae Geologicae Helvetiae, v. 84, p. 1–31.

Ionov, D.A., O'Reilly, S.Y., and Griffin, W.L., 1997, Volatile-bearing minerals and lithophile trace elements in the upper mantle: Chemical Geology, v. 141, p. 153–184.

Jahn, B., and Zhang, Z.Q., 1984, Archean granulite gneisses from eastern Hebei Province, China: Rare earth geochemistry and tectonic implications: Contributions to Mineralogy Petrology, v. 85, p. 224–243.

Jahn, B.M., Chen, B., Li, H.Y., and Potel, S., 2001, Continental subduction and mantle metasomatism: Consequence on the cretaceous magmatism and implications for the architecture of the Dabie Orogen, *in* UHPM Work shop at Waseda University, Japan, August, p. 30–31.

Jahn, B.M., Wu, F.Y., and Luo, C.H., 1999, Crust-mantle interaction induced by deep subduction of the continental crust: Geochemical and Sr-Nd isotopic evidence from post-collisional mafic-ultramafic intrusion of the northern Dabie Complex, central China: Chemical Geology, v. 157, p. 119–146.

Ji, S.C., Wang, Q., and Xu, Z.Q., 2008, Break-up of the North China Craton through lithospheric thinning: Acta Geologica Sinica, v. 82, p. 174–193 (in Chinese with English abstract).

Jing, L.Z., Guo, J.Y., and Ding, C.X., 1995, Geochronology and origin of Saima alkaline rocks in Liaoning Province: Liaoning Geology, v. 4, p. 257–271 (in Chinese with English abstract).

Johnson, K.T.M., 1998, Experimental determination of partition coefficients for rare earth and high-field-strength elements between clinopyroxene, garnet, and basaltic melt at high pressures: Contributions to Mineralogy and Petrology, v. 133, p. 60–68.

Johnson, M.C., and Plank, T., 1999, Dehydration and melting experiments constrain the fate of subducted sediments: Geochemistry Geophysics Geosystems, v. 1, p. 1007, doi: 10.1029/1999GC000014.

Li, J.H., He, W.Y., and Qian, X.L., 1997, Genetic mechanism and tectonic setting of Proterozoic mafic dyke swarm: Its implication for Paleoplate reconstruction: Geological Journal of Chinese Universities, v. 3, p. 272–280 (in Chinese with English abstract).

Li, J.Y., 2006, Permian geodynamic setting of Northeast China and adjacent regions: Closure of the Paleo-Asian Ocean and subduction of the Paleo-Pacific Plate: Journal of Asian Earth Sciences, v. 26, p. 207–224.

Li, W.P., Lu, F.X., Li, X.H., Zhou, Y.Q., and Zhang, D.G., 2001, The origin of early cretaceous volcanic rocks of Yixian formation and crust-mantle interaction in west Liaoning Province, eastern China: Journal of Mineralogy and Petrology, v. 21, p. 1–6 (in Chinese with English abstract).

Lin, W., Faure, M., and Nomade, S., 2008, Permian-Triassic amalgamationof Asia: Insights from Northeast China sutures and their place in the final collision of North China and Siberia: Comptes Rendus Geoscience, v. 340, p. 190–201.

Liu, D.Y., Nutman, A.P., and Compston, W., 1992, Remnants of ≥3800 Ma crust in the Chinese part of the Sino-Korean craton: Geology, v. 20, p. 339–342.

Liu, S., Hu, R.Z., Feng, G.Y., Yang, Y.H., Feng, C.X., Qi, Y.Q., and Wang, T., 2010a, Distribution and significance of the mafic dyke swarms since Mesozoic in North China Craton: Geological Bulletin of China, v. 29, no. 2–3, p. 1–9 (in Chinese with English abstract).

Liu, S., Hu, R.Z., Gao, S., Feng, C.X., Qi, L., Zhong, H., Xiao, T.F., Qi, Y.Q., Wang, T., and Coulson, I.M. 2008a, Zircon U-Pb geochronology and major, trace elemental and Sr-Nd-Pb isotopic geochemistry of mafic dykes in western Shandong Province, east China: Constrains on their petrogenesis and geodynamic significance: Chemical Geology, v. 255, p. 329–345.

Liu, S., Hu, R.Z., Zhao, J.H., and Feng, C.X., 2004, K–Ar geochronology of Mesozoic mafic dikes in Shandong Province, Eastern China: Implications for crustal extension: Acta Geologica Sinica, v. 78, p. 1207–1213 (in Chinese with English abstract).

Liu, S., Su, W.C., Hu, R.Z., Feng, C.X., Gao, S., Coulson, I.M., Wang, T., Feng, G.Y., Tao, Y., and Xia, Y., 2010b, Geochronological and geochemical constraints on the petrogenesis of alkaline ultramafic dykes from southwest Guizhou Province, SW China: Lithos, v. 114, p. 253–264.

Liu, S., Zou, H.B., Hu, R.Z., Zhao, J.H., and Feng, C.X., 2006, Mesozoic mafic dikes from the Shandong Peninsula, North China Craton: Petrogenesis and tectonic implications: Geochemical Journal, v. 40, p. 181–195 (in Chinese with English abstract).

Liu, Y.S., Gao, S., Hu, Z., Gao, C., Zong, K., and Wang, D., 2010c, Continental and oceanic crust recycling-induced melt-peridotite interactions in the Trans-North China Orogen: U-Pb dating, Hf isotopes and trace elements in zircons of mantle xenoliths: Journal of Petrology, v. 51, p. 537–571.

Liu, Y.S., Gao, S., and Luo, T.C., 1999, Geochemistry of granulites in North China Craton: Implications for the composition of archean lower crust: Geology Geochemistry, v. 27, no. 3, p. 40–46.

Liu, Y.S., Hu, Z., Zong, K., Gao, C., Gao, S., Xu, J., and Chen, H., 2010d, Reappraisement and refinement of zircon U-Pb isotope and trace element analyses by LA-ICP-MS: Chinese Science Bulletin, v. 55, p. 1535–1546.

Liu, Y.S., Hu, Z.C., Gao, S., Günther, D., Xu, J., Gao, C.G., and Chen, H.H., 2008b, In situ analysis of major and trace elements of anhydrous minerals by LA-ICP-MS without applying an internal standard: Chemical Geology, v. 257, p. 34–43.

Ludwig, K.R., 2003, ISOPLOT 3.00: A Geochronological Toolkit for Microsoft Excel: Berkeley, Berkeley Geochronology Center, California.

Lugmair, G.W., and Harti, K., 1978, Lunar initial $^{143}Nd/^{144}Nd$: Differential evolution of the lunar crust and mantle: Earth Planetary Science Letters, v. 39, p. 349–357.

Ma, C., Li, Z., Ehlers, C., Yang, K., and Wang, R., 1998, A post-collisional magmatic plumbing system: Mesozoic granitoid plutons from the Dabieshan high-pressure and ultrahigh-pressure metamorphic zone, east-central China: Lithos, v. 45, p. 431–456.

Ma, Q., and Zheng, J.P., 2009, In-situ U-Pb dating and Hf isotopic analyses of zircon in the volcanic rock of the Lanqi formation in the Beipiao area, western Liaoning Province: Acta Petrologica Sinica, v. 25, 3287–3297 (in Chinese with English abstract).

Macdonald, R., Rogers, N.W., and Fitton, J.G., 2001, Plume-lithosphere interactions in the generation of the basalts of the Kenya rift, East Africa: Journal of Petrology, v. 42, p. 877–900.

McKenzie, D., and O'Nions, R.K., 1991, Partial melts distributions from inversion of rare earth element concentrations: Journal of Petrology, v. 32, p. 1021–1091.

Menzies, M.A., Fan, W.M., and Zhang, M., 1993, Palaeozoic and Cenozoic lithoprobes and the loss of >120 km of Archean lithosphere, Sino-Korean craton, China, *in*: Prichard, H.M., *et al*., *eds*., Magmatic processes and plate tectonics: Geological Society of London, Special Publications, v. 76, p. 71–81.

Miao, L.C., Zhang, F.Q., and Fan, W.M., 2007, Phanerozoic evolution of the Inner Mongolia – Daxinganling orogenic belt in North China: Constraints from geochronology of ophiolites and associated formations: Geological Society of London, Special Publications, v. 280, p. 223–237.

Mohr, P.A., 1987, Crustal Contamination in mafic sheets: A summary, *in*: Halls, H.C., Fahrig, W.C., eds., Mafic dyke Swarms: Geological Association of Canada, Special Publications, v. 34, p. 75–80.

Mu, B.L., and Yan, G. H., 1992, Geological features of Triassic alkaline and subalkaline igneous comp lexes in the Yan-Liaoarea: Acta Geologica Sinica, v. 5, p. 339–355 (in Chinese with English abstract).

Münker, C., 2000, The isotope and trace element budget of the Cambrian Devil River Arc System, New Zealand: Identification of four source components: Journal of Petrology, v. 41, p. 759–788.

Ni, Z.Y., Zhai, M.G., and Wang, R.M., 2004, Discovery of Late Paleozoic retrograded eclogites from the middle part of the northern margin of North China Craton: Chinese Science Bulletin, v. 49, p. 600–606 (in Chinese with English abstract).

Pearce, J.W., and Peate, D.W., 1995, Tectonic implications of the composition of volcanic arc magmas: Annual Review of Earth and Planetary Sciences, v. 23, p. 251–285.

Potts, P.J., and Kane, J.S., 2005, International association of geoanalysts certificate of analysis: Certified reference material OU-6 (Penrhyn slate): Geostandards and Geoanalytical Research, v. 29, p. 233–236.

Qi, L., and Conrad Grégoire, D., 2002, Determination of trace elements in twenty six Chinese geochemistry reference materials by inductively coupled plasma-mass spectrometry: The Journal of Geostandards and Geoanalysis, v. 24, p. 51–63.

Rapp, R.P., and Watson, E.B., 1995, Dehydration melting of metabasalt at 8–32 kbar: Implications for continental growth and crust-mantle recycling: Journal of Petrology, v. 36, p. 891–931.

Regelous, M., Collerson, K.D., Ewart, A., and Wendt, J.I., 1997, Trace element transport rates in subduction zones: Evidence from Th, Sr and Pb isotope data for Tonga-Kermadec arc lavas: Earth Planetary Science Letter, v. 150, p. 291–302.

Ren, K.X.,Yan, G.H., Mu, B.L., Xu, B.L., Tong, Y., Chen, T.L., and Cai, J.H., 2005, Rb-Sr age and geological implication of the Alxa alkaline-rich intrusive rocks, Western Inner Mongolia: Acta Scientiarum Naturalium Universitatis Pekinensis, v. 41, p. 204–211 (in Chinese with English abstract).

Ren, S.M., and Huang, B.C., 2002, Preliminary study on post-late Paleozoic kinematics of the main blocks of the paleo-Asian Ocean: Progress in Geophsics, v. 17, p. 113–120 (in Chinese with English abstract).

Sengör, A.M.C., Natal'in, B.A., and Burtman, V.S., 1993, Evolution of the Altaid tectonic collage and Paleozoic crustal growth in Eurasia: Nature, v. 364, p. 299–307.

Shang, Q.H., 2004, Occurrences of Permian radiolarians in central and eastern Nei Mongol (Inner Mongolia) and their geological significance to the Northern China Orogen: Chinese Science Bulletin, v. 49, p. 2574–2579 (in Chinese with English abstract).

Shao, J.A., Han, Q.J., and Zhang, L.Q., 1999, Found of the xenoliths from Early Mesozoic accumulational complex in the eastern Inner Mongolia: Chinese Science Bulletin, v. 44, p. 478–485 (in Chinese with English abstract).

Shao, J.A., Zhang, Y.B., and Zhang, L.Q., 2003, Early Mesozoic dyke swarms of carbonatites and lamprophyres in Datong area: Acta Petrologica Sinica, v. 19, p. 93–104 (in Chinese with English abstract).

Shi, Y.R., Liu, D.Y., and Zhang, Q., 2004, SHRIMP dating of diorites and granites in southern Suzuoqi, Inner Mongolia: Acta Geologica Sinica, v. 78, p. 789–799 (in Chinese with English abstract).

Steiger, R.H., and Jäger, E., 1977, Subcommission on geochronology: Convention on the use of decay constants in geochronology and cosmochronology: Earth Planetary Science Letters, v. 36, p. 359–362.

Sun, S.S., and McDonough, W.F., 1989, Chemical and isotopic systematics of oceanic basalts: Implications for mantle composition and processes, *in*: Saunders, A.D., Norry, M.J., eds., Magmatism in the Ocean Basins: Geological Society Special Publication, London, p. 313–345.

Taylor, S.R., and McLennan, S.M., 1985, The continental crust: Its composition and evolution: Blackwell: Oxford, p. 312.

Thompson, M., Potts, P.J., Kane, J.S., and Wilson, S., 2000, An international proficiency test for analytical geochemistry laboratories-report on round 5 (August 1999): Geostandards and Geoanlytical Research, 24, p. E1–E28.

Tian, W., Chen, B., Liu, C.Q., and Zhang, H.F., 2007, Zircon U-Pb age and Hf isotopic composition of the Xiaozhangjiakou ultramafic pluton in northern Hebei: Acta petrologica sinica, v. 23, p. 583–590.

Wang, D.Z., Ren, Q.J., Qiu, J.S., Chen, K.R., Xu, Z.W., and Zen, J.H., 1996, Characteristics of volcanic rocks in the shoshonite province, eastern China, and their metallogenesis: Acta Geologica Sinica, v. 70, p. 23–34.

Wang, H., and Mo, X., 1995, An outline of the tectonic evolution of China: Episodes, v. 18, p. 6–16.

Wang, Q., Liu, X.Y., and Li, J.Y., 1991, Plate tectonics between Cathaysia and Angaraland in China, *in*: Tang Kedong, *et al*., eds., Special papers on the plate tectonics of northern China No. 4: Beijing, Peking University Publishing House, p. 56–60 (in Chinese with English abstract).

Wang, X., Griffin, W.L., Wang, Z., and Zhou, X.M., 2003, Hf isotope compositions of zircons and implications for the petrogenesis of Yajiangqiao granite, Hunan Province, China: Chinese Science Bulletin, v. 48, p. 995–998.

Wiedenbeck, M., Alle, P., Corfu, F., Griffin, W.L., Meier, M., Oberli, F., Quadt, A.V., Roddick, J.C., and Spiegel, W., 1995, Three natural zircon standards for U-Th-Pb, Lu-Hf, trace element and REE analyses: Geostandards and Geoanalytical Research, v. 19, p. 1–23.

Windley, B.F., 1984, The evolving continents: John Wiley & Sons, p. 68–218.

Windley, B.F., Alexeiev, D., and Xiao, W.J., 2007, Tectonic models for accretion of the Central Asian Orogenic Belt: Journal of the Geological Society London, v. 164, p. 31–48.

Wood, D.A., Tarneu, J., Varet, J., Saunders, A.N., Bouhault, H., Joron, J.L., Treuil, M., and Cann, J.R., 1979, Geochemistry of basalts drills in the North Atlantic by IPOD Leg 49: Implications for mantle heterogeneity: Earth Planetary Science Letters, v. 42, p. 77–97.

Wu, F.Y., Jahn, B.M., and Lin, Q., 1997, Isotopic characteristics of the post-orogenic granite in orogenic belt of Northern China and their implications for crustal growth: Chinese Science Bulletin, v. 42, p. 2188–2191 (in Chinese with English abstract).

Wu, F.Y., Jahn, B.M., Wilde, S.A., and Sun, D.Y., 2000, Phanerozoic continental crustal growth: U-Pb and Sr-Nd isotopic evidence from the granites in northeastern China: Tectonophysics, v. 328, p. 89–113.

Wu, F.Y., Lin, J.Q., and Wilde, S.A., 2005, Nature and significance of the Early Cretaceous giant igneous event in eastern China: Earth and Planetary Science Letters, v. 233, p. 103–119.

Wu, F.Y., Walker, R.J., Ren, X.W., Sun, D.Y., and Zhou, X.H., 2003, Osmium isotopic constraints on the age of lithospheric mantle beneath northeastern China: Chemical Geology, v. 197, p. 107–129.

Wu, F.Y., Walker, R.J., Yang, Y.H., Yuan, H.L., and Yang, J.H., 2006, The chemical–temporal evolution of lithospheric mantle underlying the North China Craton: Geochimica et Cosmochimica Acta, v. 70, p. 5013–5034.

Wu, F.Y., Xu, Y.G., Gao, S., and Zheng, J.P., 2008, Lithospheric thinning and destruction of the North China Craton: Acta Petrologica Sinica, v. 24, p. 1145–1174 (in Chinese with English abstract).

Wu, F.Y., Ye, M., and Zhang, S.H., 1995, The geodynamic model of the Manzhouli-Suifenhe geoscience transect: Journal of Earth Science, v. 20, p. 535–539 (in Chinese with English abstract).

Wu, F.Y., Zhao, G.C., and Sun, D.Y., 2007, The Hulan Group: Its role in the evolution of the Central Asian Orogenic Belt of NE China: Journal of Asian Earth Sciences, v. 30, p. 542–556.

Xiao, W., Windley, B.F., Hao, J., and Zhai, M.G., 2003, Accretion leading to collision and the Permian Solonker suture, Inner Mongolia, China: Termination of the central Asian orogenic belt: Tectonics, v. 22, p. 1069, doi: 10.1029/2002TC001484.

Xiao, W.J., Windley, B.F., and Huang, B.C., 2009, End-Permian to mid-Triassic termination of the accretionary processes of the southernAltaids: Implications for the geodynamic evolution, Phanerozoic continental growth, and metallogeny of Central Asia: International Journal of Earth Sciences, v. 98, p. 1189–1217.

Xu, Y.G., 2001, Thermo-tectonic destruction of the Archean lithospheric keel beneath the Sino-Korean Craton in China: Evidence, timing and mechanism: Physics and Chemistry of the Earth (A), v. 26, p. 747–757.

Xu, Y.G., Huang, X.L., and Ma, J.L., 2004, Crust-mantle interaction during the tectono-thermal reactivation of the North China craton: Constraints from SHRIMP zircon U-Pb chronology and geochemistry of Mesozoic plutons from western Shandong: Contributions to Mineralogy and Petrology, v. 147, p. 750–767.

Xu, Y.G., Li, H.Y., Pang, C.J., and He, B., 2009, On the timing and duration of the destruction of the North China Craton: Chinese Science Bulletin, v. 54, p. 3379–3396.

Yan, G.H., Mu, B.L., and Xu, B.L., 2000, Geochronology and Sr-Nd-Pb isotopic characteristics and significance of the Triassic alkaline intrusions from the Yanliao-Yinshan area: Science in China (D), v. 30, p. 383–387 (in Chinese with English abstract).

Yan, G.H., Mu, B.L., Xu, B.L., He, G.Q., Han, B.F., Wang, S.G., Tong, Y., Ren, K.X., Yang, B., Hong, D.W., Qiao, G.S., Xu, R.H., Zhang, R.H., and Chu, Z.Y., 2001, Characteristics and implication of Nd, Sr and Pb isotopes and chronology of Phanerozoic alkaline-rich intrusions in North China: Geological Review, v. 48, p. 69–76 (in Chinese with English abstract).

Yang, J.H., Wu, F.Y., and Wilde, S.A., 2003, A review of the geodynamic setting of large-scale Late Mesozoic gold mineralization in the North China Craton: An association with lithospheric thinning: Ore Geology Reviews, v. 23, p. 125–152.

Yang, W., 2007, Geochronology and geoehemistry of the Mesozoie volcanic rocks in Wstern Liaoning: constraintson mechanism for the lithospheric thinning in the North China Craton: Guangzhou, Guangzhou Institute of Geochemistry, Chinese Academy of Sciences (in Chinese with English abstract).

Yang, W., and Li, S.G., 2008, Geochronology and geochemistry of the Mesozoic volcanic rocks in Western Liaoning: Implications for lithospheric thinning of the North China Craton: Lithos, v. 102, p. 88–107.

Ye, M., Zhang, S.H., and Wu, F.Y., 1994, The classification of the Paleozoic tectonic units in the area crossed by Manzhouli-Suifenghe geoscience transects: Journal of Changchun University Earth Science, v. 24, p. 241–245 (in Chinese with English abstract).

Zhai, M.G., 2008a, State of lithosphere beneath the North China Craton before the Mesozoic lithospheric disruption: A suggestion: Geotectonica Et Metallogenia, v. 32, p. 516–520 (in Chinese with English abstract).

Zhai, M.G., 2008b, Lower crust and lithospheric mantle beneath the North China Craton before the Mesozoic lithospheric disruption: Acta Petrologica Sinica, v. 24, p. 2185–2204 (in Chinese with English abstract).

Zhai, M.G., Fan, H.R., Yang, J.H., and Miao, L.C., 2004, Large-scale cluster of gold deposits in east Shandong: Anorogenic metallogenesis: Earth Science Frontiers (China University of Geosciences, Beijing), v. 11, no. 1, p. 85–97 (in Chinese with English abstract).

Zhang, C.H., 2009a, Selected tectonic topics in the investigation of geodynamic process of destruction of North China craton: Earth Science Frontiers, v. 6, p. 203–214 (in Chinese with English abstract).

Zhang, H., Liu, X.M., Chen, W., Li, Z.T., and Yang, F.L., 2005a, The age of the top of the Yixian Formation in the Beipiao-Yixian area, western Liaoning, and its importance: Geology in China, v. 32, p. 596–603 (in Chinese with English abstract).

Zhang, H., Liu, X.M., Yuan, H.L., Hu, Z.C., and Diwu, C.R., 2006, U-Pb isotopic age of the lower Yixian formation in Lingyuan of Western Liaoning and its significance: Geology Review, v. 52, p. 63–71 (in Chinese with English abstract).

Zhang, H., Sun, M., Zhou, X., Zhou, M., Fan, W., and Zheng, J., 2003, Secular evolution of the lithosphere beneath the eastern North China Craton: Evidence from Mesozoie basalts and high-Mg andesites: Geoehimica et Cosmochimica Acta, v. 67, p. 4373–4387.

Zhang, H.F., 2009b, Peridotite-melt interaction: A key point for the destruction of cratonic lithospheric mantle: Chinese Science Bulletin, v. 54, p. 3417–3437.

Zhang, H.F., Sun, M., Zhou, X.H., Fan, W.M., Zhai, M.G., and Yin, J.F., 2002, Mesozoic lithosphere destruction beneath the North China Craton: Evidence from major-, traceelement and Sr-Nd-Pb isotope studies of Fangcheng basalts: Contributions to Mineralogy and Petrology, v. 144, p. 241–253.

Zhang, H.F., Sun, M., and Zhou, M.F., 2004, Highly heterogeneous Late Mesozoic lithospheric mantle beneath the North China Craton: Evidenee from Sr-Nd-Pb isotopic systematics of mafic igneous rocks: Geological Magazine, v. 141, p. 55–62.

Zhang, H.F., Sun, M., Zhou, X.H., and Ying, J.F., 2005b, Geochemical constraints on the origin of Mesozoic alkaline intrusive complexes from the North China Craton and tectonic implications: Lithos, v. 81, p. 297–317.

Zhang, H.F., and Yang, Y.H., 2007, Emplacement age and Sr-Nd-Hf isotopic characteristics of the diamondiferous kimberlites from the eastern North China Craton: Acta Petrologica Sinica, v. 23, p. 285–294 (in Chinese with English abstract).

Zhang, S.H., Zhao, Y., and Song, B., 2006b, Hornblende therobarometry of the Carboniferous granitoids from the Inner Mongolia Paleo-uplift: Implications for the geotectonic evolution of the northern margin of North China block: Mineralogy and Petrology, v. 87, p. 123–141.

Zhang, S.H., Zhao, Y., Liu, X.C., Liu, D.Y., Chen, F.K., Xie, L.W., and Chen, H.H., 2009, Late Paleozoic to Early Mesozoic mafic–ultramafic complexes from the northern North China Block: Constraints on the composition and evolution of the lithospheric mantle: Lithos, v. 110, p. 229–246.

Zhang, S.H., Zhao, Y., Liu, J.M., Hu, J.M., Song, B., Liu, J., and Wu, H., 2010, Geochronology, geochemistry and tectonic setting of the Late Paleozoic-Early Mesozoic magmatism in the northern margin of the North China Block: A preliminary review: Acta Petrologica Et Mineralogica, v. 29, p. 824–842 (in Chinese with English abstract).

Zhang, S.H., Zhao, Y., and Song, B., 2007a, Petrogenesis of the Middle Devonian Gushan diorite pluton on the northern margin of the North China block and its tectonic implications: Geological Magazine, v. 144, p. 553–568.

Zhang, S.H., Zhao, Y., and Song, B., 2007b, Carboniferous granitic plutons from the northern margin of the North China block: Implications for a late Paleozoic active continental margin: Journal of the Geological Society London, v. 164, p. 451–463.

Zhang, S.H., Zhao, Y., and Song, B., 2007c, Zircon SHRIMP U-Pb and insitu Lu-Hf isotope analyses of a tuff from Western Beijing: Evidence for missing late Paleozoic arc volcano

eruption at the northern margin of the North China block: Gondwana Research, v. 12, no. 1–2, p. 157–165.

Zhao, J.H., and Zhou, M.F., 2007, Geochemistry of neoproterozoic mafic intrusions in the Panzhihua district (Sichuan Province, SW China): Implications for subduction related metasomatism in the upper mantle: Precambrian Research, v. 152, p. 27–47.

Zhao, X.X., Coe, R.S., Zhou, Y.X., Wu, H.R., and Wang, J., 1990, New plaeomagnetic results from northern China: Collision and suturing with Siberia and Kazakstan: Tectonophysics, v. 181, p. 43–81.

Zhao, Y., Chen, B., Zhang, S.H., Liu, J.M., Hu, J.M., Liu, J., and Pei, J.L., 2010, Pre-Yanshanian geological events in the northern margin of the North China Craton and its adjacent areas: Geology in China, v. 7, p. 900–915 (in Chinese with English abstract).

Zheng, J.P., 1999, Mesozoic–Cenozoic Mantle Replacement and Lithospheric Thinning beneath the Eastern China: Wuhan, China University of Geosciences Press, p. 126 (in Chinese with English summary).

Zheng, J.P., 2009, Comparison of mantle-derived matierals from different spatiotemporal settings: Implications for destructive and accretional processes of the North China Craton: Chinese Science Bulletin, v. 54, p. 3397–3416.

Zheng, J.P., and Lu, F.X., 1999, Mantle xenoliths from kimberlites, Shandong and Liaoning: Paleozoic mantle character and its heterogeneity: Acta Petrologica Sinica, v. 15, p. 65–74 (in Chinese with English abstract).

Zheng, Y.F., and Wu, F.Y., 2009, Growth and reworking of cratonic lithosphere: Chinese Science Bulletin, v. 54, p. 3347–3353.

Zhou, D.W., Zhang, C.L., and Liu, Y.Y., 1998, Study on basic dyke swarms developed in the basement in the continental orogen: An example from Wudang block in Southern Qinling: Advance in Earth Sciences, v. 13, p. 151–156 (in Chinese with English abstract).

Zhou, X.H., 2006, Major transformation of subcontinental lithosphere beneath eastern China in the Cenozoic-Mesozoic: Review and prospect: Earth Science Frontiers, v. 13, p. 50–54 (in Chinese with English abstract).

Zhou, X.H., Zhang, G.H., Yang, J.H., Chen, W.J., and Sun, M., 2001, Sr-Nd-Pb isotope mapping of late Mesozoic volcanic rocks across northern margin of North China Craton and implications to geodynamic processes: Geochimica, v. 30, p. 10–23 (in Chinese with English abstract).

Zhou, X.H., Zhang, H.F., Ying, J.F., and Chen, L.H., 2005, Geochemical records of subsequent effects of continental deep subduction: Discussion of mantle source variations of the Mesozoic lithospheric mantle of the North China Craton: Acta Petrologica Sinica, v. 21, p. 1255–1264 (in Chinese with English abstract).

Zhu, G., Song, C.Z., Wang, D.X., Liu, G.S., and Xu, J.W., 2001a, Studies on 40Ar/39Ar thermo chronology of strike-slip time of the Tan-Lu fault zone and their tectonic implications: Science in China (D), v. 44, p. 1002–1009.

Zhu, G., Wang, D.X., Liu, G.S., Song, C.Z., Xu, J.W., and Niu, M.L., 2001b, Extensional activities along the Tan-Lu fault zone and its geodynamic setting: Chinese Journal of Geology, v. 36, p. 269–278(in Chinese with English abstract).

Zhu, R.X., and Zheng, T.Y., 2009, Destruction geodynamics of the North China Craton and its Paleoproterozoic plate tectonics: Chinese Science Bulletin, v. 54, p. 3354–3366.

Zorin, Y.A., Belichenko, V.G., and Turuzantov, E.K, 1993, The south Siberia-central Mongolia transect: Tectonophysics, v. 225, p. 361–378.